NUMERICAL STUDY OF OSCILLATORY FLOW PAST FOUR CYLINDERS IN SQUARE ARRANGEMENT

P. Anagnostopoulos, Ch. Dikarou and S. Seitanis
Aristotle University of Thessaloniki,
Department of Civil Enfineering,
Thessaloniki 54124, Greece

ABSTRACT

The results of a numerical study of the viscous oscillating flow around four circular cylinders are presented herein, for a constant frequency parameter, β, equal to 50, and Keulegan-Carpenter numbers, KC, ranging between 0.2 and 10. The cylinders were placed on the vertices of a square with two sides normally and two parallel to the oncoming flow, for a pitch ratio, P/D, equal to 2. The finite-element method was employed for the solution of the Navier-Stokes equations, in the formulation where the stream function and the vorticity are the field variables. The streamlines and the vorticity contours generated from the solution were used for the flow visualization. At low values of the Keulegan-Carpenter number the flow remains symmetrical with respect to the horizontal axis of symmetry of the solution domain. As the Keulegan-Carpenter number is increased to 4 the flow becomes aperiodic at consecutive cycles. For KC equal to 6 asymmetries appear in the flow, which are eventually amplified as KC increases still further. These asymmetries, in association with the aperiodicity at different cycles, lead to an almost chaotic configuration, as KC grows larger. For characteristic cases the flow pattern and the traces of the hydrodynamic forces are presented, whereas the mean and r.m.s. values of the in-line and transverse forces and the coefficients of the in-line force were evaluated for the entire range of Keulegan-Carpenter numbers examined.

1. INTRODUCTION

Oscillatory flow past a circular cylinder has attracted the interest of researchers in recent years, since it provides a simplified tool for the simulation of flow around a cylinder immersed in a wave environment. The phenomenon is controlled by two dimensionless numbers; the Keulegan-Carpenter number, $KC=U_mT/D$, and the Reynolds number, $Re=U_mD/v$, where U_m is the maximum flow velocity, T the period of oscillation, D the cylinder diameter and v the kinematic viscosity of the fluid. The ratio of these two numbers, $\beta=Re/KC=D^2/vT$, is defined as the frequency parameter.

Although numerous experimental and computational studies for oscillatory flow past a single cylinder are quoted in the literature, information of oscillatory flow past two or more cylinders is scarce. Oscillatory flow past two cylinders was examined experimentally by Williamson (1985) and computationally by Skomedal *et al.* (1989), in studies comprising also the investigation of oscillatory flow past a single cylinder. Anagnostopoulos *et al.* have studied numerically the oscillatory flow past two cylinders in a side-by-side arrangement for P/D=1.2 (2002) and P/D=2 (2005), and in oblique arrangement for P/D=1.41 (2003).

In the present study the computational simulation of viscous oscillatory flow past four circular cylinders is conducted, using the finite-element technique. The cylinders were placed on the vertices of a square with two sides normally and two parallel to the oncoming flow, for a pitch ratio, P/D, equal to 2. The frequency parameter was held constant equal to 50, whereas the Keulegan-Carpenter numbers were varied between 0.2 and 10. The numerical solution provides a complete description of both the flow field and the hydrodynamic forces exerted on the cylinders. The vorticity contours were used mainly for the flow visualization, whereas the streamlines are shown in a few cases. The mean and r.m.s. values of the hydrodynamic forces and the coefficients of the in-line force were evaluated for the KC numbers considered herein and are presented in diagrams.

2. THE NUMERICAL SOLUTION

In the present study the formulation of the Navier-Stokes equations is employed, in which the stream function, Ψ, and the vorticity, ζ, are the field variables. In this formulation the Navier-Stokes equations are written as:

$$\nabla^2 \Psi = -\zeta \qquad (1)$$

$$\frac{\partial \zeta}{\partial t}+\frac{\partial \Psi}{\partial y}\frac{\partial \zeta}{\partial x}-\frac{\partial \Psi}{\partial x}\frac{\partial \zeta}{\partial y}=\nu\nabla^2\zeta \qquad (2)$$

The pressure distribution throughout the solution domain was obtained from the solution of Poisson's equation

$$\nabla^2 p=-2\rho\left(\frac{\partial u}{\partial y}\frac{\partial v}{\partial x}-\frac{\partial u}{\partial x}\frac{\partial v}{\partial y}\right) \qquad (3)$$

where ρ is the fluid density.

The time-dependent free stream velocity $U(t)$ of the oscillatory flow is defined in terms of the maximum flow velocity, U_m, as

$$U(t)=U_m\sin\varphi, \qquad \varphi=2\pi t/T \qquad (4)$$

where t is the time interval elapsed from the inception of the flow oscillation.

The numerical technique is described in full detail by Iliadis and Anagnostopoulos (1998). The solution of equations (1) to (3) yields the distribution of stream function, vorticity and pressure in the solution domain.

From the distribution of pressure and shear on each cylinder the in-line and transverse forces per unit cylinder length, F_x^* and F_y^*, were evaluated. These forces were non-dimensionlized by

$$F_x=F_x^*/(0.5\,\rho\,U_m^2\,D) \text{ and } F_y=F_y^*/(0.5\,\rho\,U_m^2\,D)$$

3. RESULTS

For various characteristic cases, the flow pattern and the time-dependent hydrodynamic forces will be presented. For relatively low *KC* values the flow field remains symmetrical with respect to the horizontal axis of symmetry of the computational domain, and periodic at consecutive oscillation cycles. If *KC* exceeds a critical threshold the periodicity of flow is not preserved at different cycles. If *KC* is increased still further asymmetries appear in the flow field. As *KC* grows larger these asymmetries are amplified and, in association with the aperiodicity at different cycles, lead to an almost chaotic configuration.

In the case of a periodic flow pattern one oscillation cycle is adequate for the interpretation of the flow field and of the hydrodynamic forces, whereas, when the flow field is aperiodic, results at different periods are necessary.

For KC≤ 2 the flow pattern is symmetrical with respect to the horizontal axis of symmetry of the computational domain, but asymmetric with respect

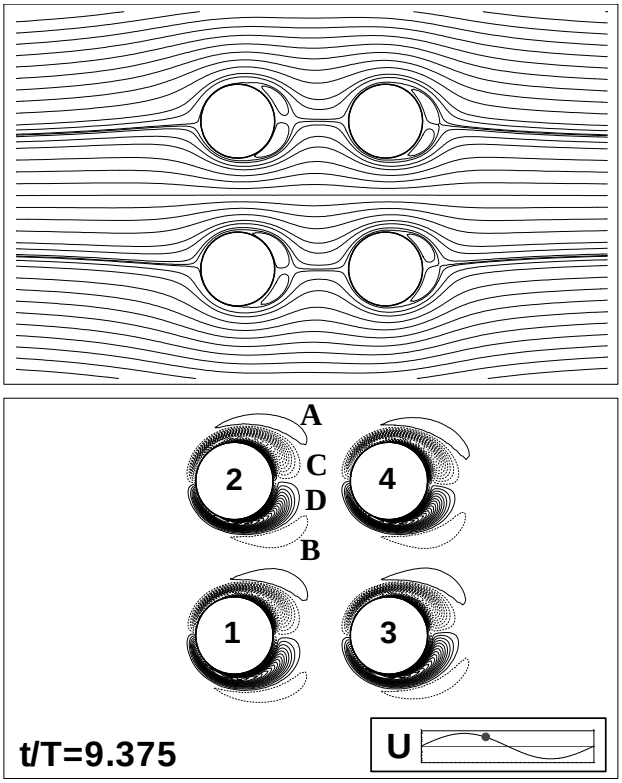

Figure 1: *Flow field for KC=2*

to the wake axis of each cylinder, due to hydrodynamic interference. Figure 1 depicts the streamlines (top) and the vorticity contours (bottom) for *KC*=2 at *t*/*T*=9.375. Small separation bubbles behind the four cylinders appear in the streamlines. The vortices C and D are forming behind cylinder 2, while vortices A and B survive from the previous half-cycle. The time-history of the hydrodynamic forces exerted on cylinder 1 for *KC*=2 are displayed in Figure 2, together with the oscillating flow velocity. The hydrodynamic forces are periodic, which is compatible to the periodicity of the flow pattern. The in-line force is sinusoidal with zero mean value, whereas the transverse force

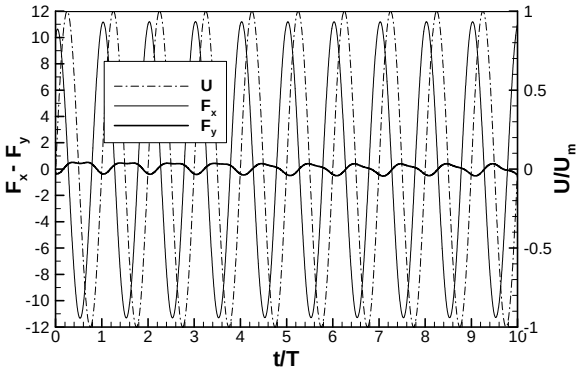

Figure 2: *Hydrodynamic forces and stream velocity for KC=2*

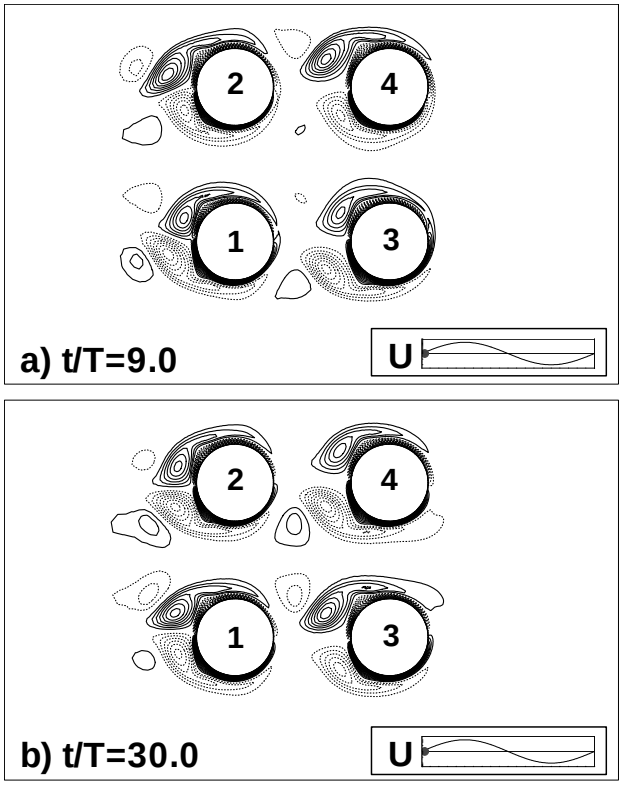

Figure 3: *Vorticity contours for KC=4*

diverges substantially from sinusoidal. The traces of the in-line forces are the same for all four cylinders. The transverse force on cylinder 2 is of

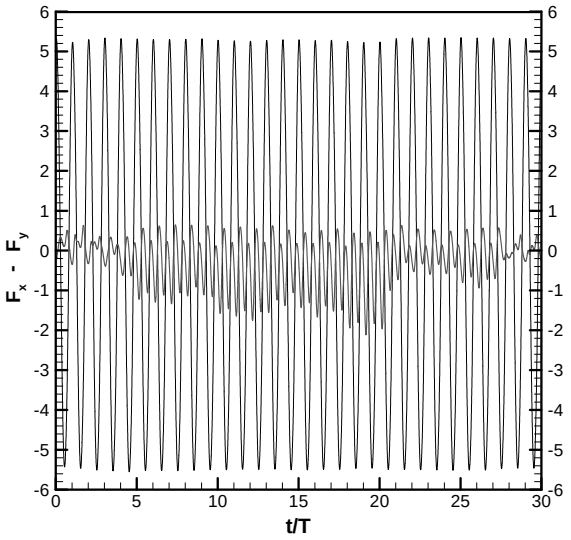

Figure 4: *Hydrodynamic forces for KC=4. F_x is shown with thin and F_y with thick line*

equal magnitude but opposite sign from that on cylinder 1, and the same applies for the transverse forces exerted on cylinders 3 and 4. The vorticity contours for *KC*=4 at *t*/*T* equal to 9 and 30 are displayed in Figure 3. At *t*/*T*=9 the outer vortices are markedly larger than the inner vortices, whereas at *t*/*T*=30 the inner vortices are larger. The aperiodicity of flow reflects on the time-history of the hydrodynamic forces. This is evident in Figure 4, which displays the hydrodynamic forces exerted

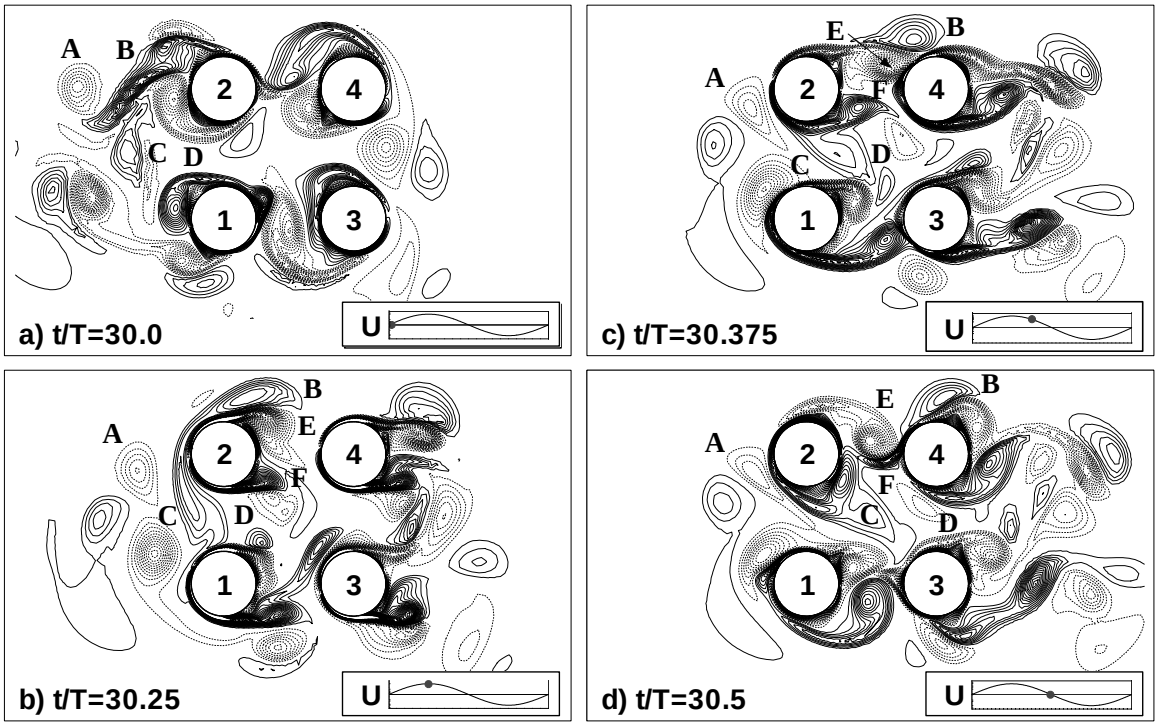

Figure 5: *Vorticity contours during a half-cycle for KC=6*

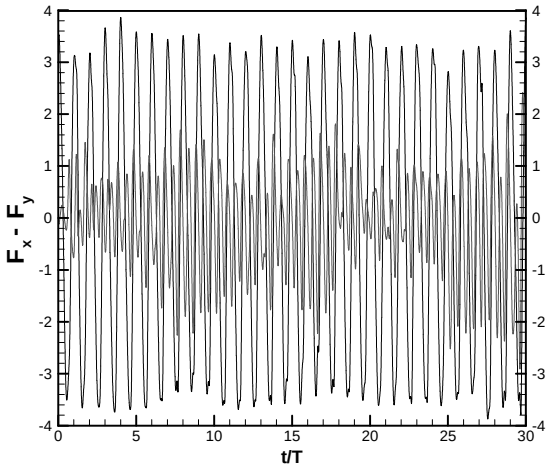

Figure 6: *Hydrodynamic forces for KC=6*

on cylinder 1 for *KC*=4. Small fluctuations are observed in the amplitude of the in-line force, whereas the aperiodicity of the transverse force is more intense. The frequency of the in-line force is equal to the frequency of the oscillatory flow, and the frequency of the transverse force equals twice the flow oscillation frequency. The transverse force on cylinder 1 is negative in the greatest part of the record.

The vorticity contours for *KC*=6 in the first half of the 31st cycle are displayed in Figure 5. In Figure 5a (*t*/*T*=30) we can detect the vortices A-B and C-D in the vicinity of cylinder 2 existing from the previous half-cycle. In the following frames vortices E and F form behind cylinder 2, vortex A comes close to this cylinder, and vortices C and D enter through the gap between the cylinders. Vortex B moves above the upper edge of cylinder 2, and pairs initially with vortex E and then with the vortex forming at the upper part of cylinder 4. The vortices formed at the outer edges of cylinders 3 and 4 at *t*/*T*=30 pair-up with the opposite-sign vortices forming at the same edges. The mutually induced velocities in the streamwise direction lead to increased displacement of the two pairs behind cylinders 3 and 4 at *t*/*T*=30.5. At the same instant the congestion of vorticity formed on cylinders 1 and 2 due to the presence of cylinders 3 and 4 is apparent. The time-history of the hydrodynamic forces exerted on cylinder 1 for *KC*=6 are displayed in Figure 6. The aperiodicity of the transverse force is more pronounced compared to that for *KC*=4. In the first fifteen cycles the mean transverse force is negative. In the interval between the 15th and 24th cycle the mean transverse force is very close to zero and it experiences a reduction in amplitude. From the 24th cycle onwards the amplitude increases and the mean transverse value becomes negative again.

The vorticity contours for *KC*=10 during the first half of the 31st cycle are shown in Figure 7.

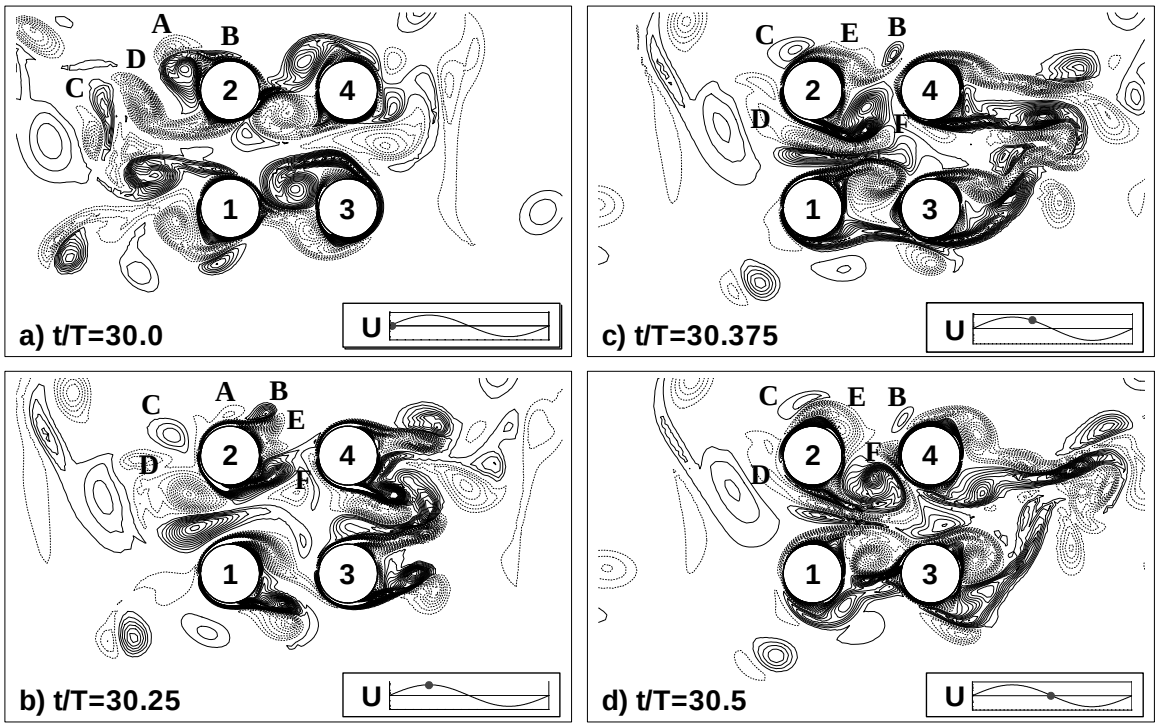

Figure 7: *Vorticity contours during a half-cycle for KC=10*

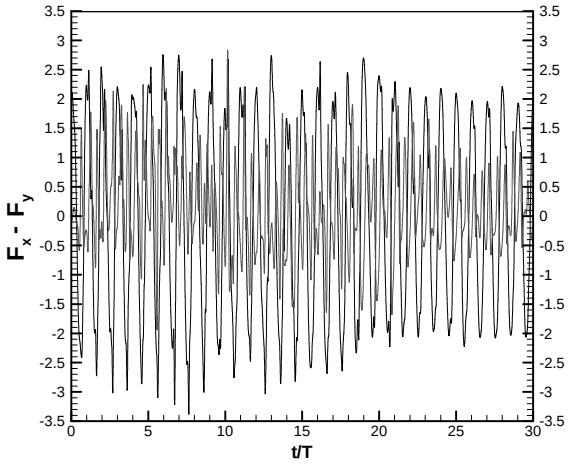

Figure 8: *Hydrodynamic forces for KC=10*

The flow pattern does not vary substantially from that for KC=6 displayed in Figure 5. The displacement of the two vortex-pairs behind cylinders 3 and 4 at t/T=30.5 is larger than those for KC=6. The time-history of the hydrodynamic forces exerted on cylinder 1 for KC=10 are displayed in Figure 8. Now both forces display a fully aperiodic character. The amplitude of the in-line force fluctuates substantially at different cycles, whereas the mean transverse force is positive in the greatest part of the record.

4. MEAN AND R.M.S. HYDRODYNAMIC FORCES - COEFFICIENTS OF THE IN-LINE FORCE

The mean value of the in-line force is practically zero. The mean value of the transverse force for the cylinders of the lower row (1 and 3) for the whole range of *KC* examined is depicted in Figure 9. The corresponding values for the two cylinders of the

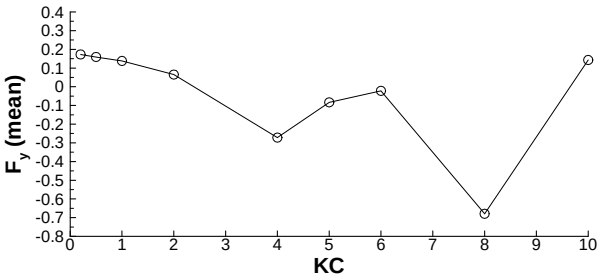

Figure 9: *Mean value of the transverse force*

upper row (2 and 4) are of equal magnitude but opposite sign. The mean transverse force decreases mildly as *KC* increases to 4 and then increases, experiencing a sudden drop when *KC* becomes equal to 8.

The r.m.s. value of the total in-line force in dimensionless form is defined as

$$F_x(r.m.s) = \left(\frac{1}{T} \int_0^T F_x^2 \, dt \right)^{1/2} \tag{5}$$

and the r.m.s. value of the fluctuation of the transverse force from the mean transverse as

$$F_y'(r.m.s) = \left(\frac{1}{T} \int_0^T F_y'^2 \, dt \right)^{1/2} \tag{6}$$

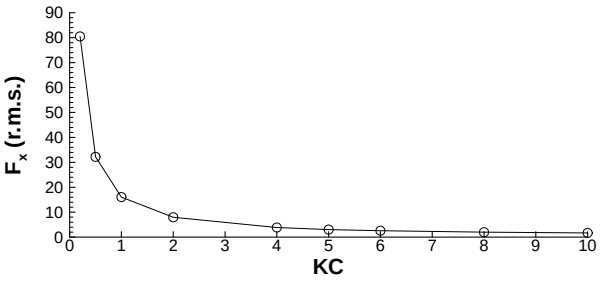

Figure 10: *R.m.s. value of the in-line force*

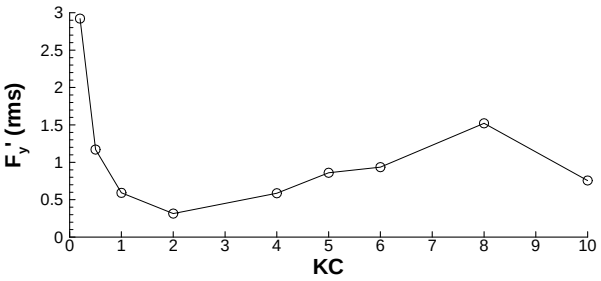

Figure 11: *R.m.s. value of the transverse force*

The r.m.s. values of the in-line and transverse forces are presented in Figures 10 and 11. F_x *(r.m.s)* decreases with increasing *KC*, the decrease being abrupt at low *KC* and mild as *KC* becomes higher than 4. The r.m.s. values of the fluctuation of the transverse force decrease as *KC* increases to 2 and then experience an increase, with a local maximum at *KC*=8.

The total in-line force exerted on a cylinder in oscillating flow can be expressed as the sum of a drag and an inertia component. The Fourier averaged drag and inertia coefficients of the in-line force derived from this decomposition, C_D and C_M, are given by

$$C_D = \frac{3}{8} \left(\int_0^{2\pi} F_x \sin\varphi \, d\varphi \right) \tag{7}$$

$$C_M = \frac{U_M T}{\pi^3 D}\left(\int_0^{2\pi} F_x \cos\varphi \, d\varphi\right) \quad (8)$$

where φ is the phase angle in Equation (4). The hydrodynamic coefficients are depicted in Figures 12 and 13.

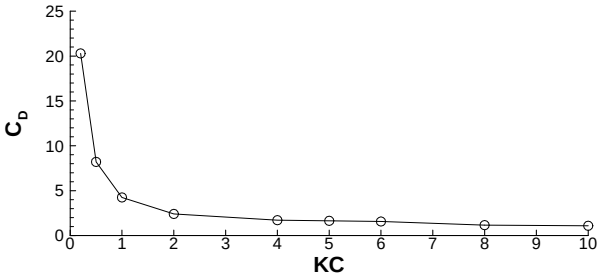

Figure 12: Drag coefficient of the in-line force

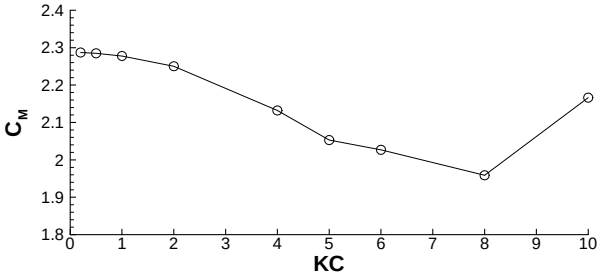

Figure 13: *Inertia coefficient of the in-line force*

Similarly to the r.m.s. value of the in-line force C_D decreases with increasing *KC*, the decrease being abrupt at low *KC* and mild as *KC* becomes higher than 4. C_M decreases gradually as *KC* increases to 8, and then increases as *KC* becomes equal to 10.

5. CONCLUSION

The finite-element study conducted herein revealed the various features of the interactive oscillating flow past four circular cylinders in square arrangement. At values of the Keulegan-Carpenter number lower than 4 the flow near the cylinders remains almost symmetrical with respect to the horizontal axis of symmetry of the solution domain. However, the flow is not symmetrical with respect to the wake axis of each cylinder, due to the interference effects. As the Keulegan-Carpenter number is increased to 4 the flow becomes aperiodic at consecutive cycles. For KC equal to 6 asymmetries appear in the flow, which are eventually amplified as KC increases still further. These asymmetries, in association with the aperiodicity at different cycles, lead to an almost chaotic configuration, as KC grows larger.

The frequency of the in-line force is equal to that of the oscillating flow, whereas the frequency of the transverse force is twice the oscillation frequency. The mean transverse force decreases mildly as *KC* increases to 4 and then increases, experiencing a sudden drop at *KC*=8. The amplitude of the in-line force exerted on the cylinders decreases with increasing *KC*, which reflects on the r.m.s. values of this force. The r.m.s. values of the fluctuation of the transverse force decrease as *KC* increases to 2 and then experience an increase, with a local maximum at *KC*=8. The drag and inertia coefficients of the in-line force decrease with increasing *KC*, more abruptly the drag coefficient and mildly the inertia coefficient.

6. REFERENCES

Anagnostopoulos, P. et al., 2002, Numerical study of oscillatory flow past pairs of cylinders at low Reynolds and Keulegan-Carpenter numbers. *In ASME 4th International Symposium on Flow-Structure Interactions, Aeroelasticity, Flow-Induced Vibration and Noise*, IMECE 2002-32178. In CD-ROM

Anagnostopoulos, P. et al., 2003, Numerical study of oscillatory flow past two cylinders in oblique arrangement. In *Computational Methods and Experimental Measurements XI* (eds C.A. Brebbia, G.M. Carlomagno & P. Anagnostopoulos), 455-464. Southampton: WIT Press.

Anagnostopoulos, P. et al., 2005, Numerical study of oscillatory flow past a pair of cylinders in a side-by-side arrangement. In *24th International Conference on Offshore Mechanics and Arctic Engineering (OMAE 2005)*, IMECE 2005-67225. In CD-ROM.

Iliadis, G., Anagnostopoulos, P., 1998, Viscous oscillatory flow around a circular cylinder at low Keulegan-Carpenter numbers and frequency parameters. *International Journal for Numerical Methods in Fluids*, **26**: 403-442.

Skomedal, N.G. et al., 1989, Viscous forces on one and two circular cylinders in planar oscillatory flow. *Applied Ocean Research*, **11**: 114-134.

Williamson, C.H.K., 1985, Sinusoidal flow relative to circular cylinders. *Journal of Fluid Mechanics*, **155**: 141-174.